Metabolic-flux analysis of Saccharomyces cerevisiae CEN.PK113-7D based on mass isotopomer measurements of 13C-labeled primary metabolites

Van Winden, Wouter A.; Van Dam, Jan C.; Ras, Cor; Kleijn, Roelco J.; Vinke, Jacobus L.; Van Gulik, Walter M.; Heijnen, Joseph J.

DOI
10.1016/j.femsyr.2004.10.007

Publication date
2005

Document Version
Final published version

Published in
FEMS Yeast Research

ELSEVIER

FEMS Yeast Research 5 (2005) 559–568

FEMS Yeast Research

www.fems-microbiology.org

Metabolic-flux analysis of *Saccharomyces cerevisiae* CEN.PK113-7D based on mass isotopomer measurements of ^{13}C-labeled primary metabolites

Wouter A. van Winden *, Jan C. van Dam, Cor Ras, Roelco J. Kleijn, Jacobus L. Vinke, Walter M. van Gulik, Joseph J. Heijnen

Kluyver Laboratory for Biotechnology, Department of Biotechnology, Faculty of Applied Sciences, Bioprocess Technology Group, Delft University of Technology, Julianalaan 67, 2628 BC Delft, The Netherlands

Received 1 August 2004; received in revised form 8 October 2004; accepted 11 October 2004

First published online 14 October 2004

Abstract

Metabolic-flux analyses in microorganisms are increasingly based on ^{13}C-labeling data. In this paper a new approach for the measurement of ^{13}C-label distributions is presented: rapid sampling and quenching of microorganisms from a cultivation, followed by extraction and detection by liquid chromatography–mass spectrometry of free intracellular metabolites. This approach allows the direct assessment of mass isotopomer distributions of primary metabolites. The method is applied to the glycolytic and pentose phosphate pathways of *Saccharomyces cerevisiae* strain CEN.PK113-7D grown in an aerobic, glucose-limited chemostat culture. Detailed investigations of the measured mass isotopomer distributions demonstrate the accuracy and information-richness of the obtained data. The mass fractions are fitted with a cumomer model to yield the metabolic fluxes. It is estimated that 24% of the consumed glucose is catabolized via the pentose phosphate pathway. Furthermore, it is found that turnover of storage carbohydrates occurs. Inclusion of this turnover in the model leads to a large confidence interval of the estimated split ratio.

Keywords: ^{13}C-labeling; Metabolic-flux analysis; *Saccharomyces cerevisiae*; LC–MS/MS; glycolysis; Pentose phosphate pathway

1. Introduction

Metabolic-flux analyses of microorganisms are increasingly based on measurements of the distribution of ^{13}C-atoms in metabolites that are derived from ^{13}C-labeled medium substrates. The measured ^{13}C-label distribution is a function of (pseudo-steady-state) intracellular fluxes and can be used to constrain metabolic fluxes when these are not fully determined by mass balances of the intracellular metabolites alone.

Recent publications on ^{13}C-labeling based-flux analyses include a number of studies on *Saccharomyces cerevisiae* strain CEN.PK113-7D. Gombert et al. [1] have used gas chromatography mass spectrometry (GC–MS) measurements of amino acids in yeast grown aerobically on 1-$^{13}C_1$-glucose to compare the fluxes in cells grown under high (batch culture) and low glucose (chemostat culture) concentrations and in cells with and without the gene coding for Mig1p, a protein known to play a role in glucose repression. Dos Santos et al. [2] have applied the same analytical and computational approach to extend the study of the central carbon metabolism of this yeast with flux analyses of the same strain, and an isogenic malic enzyme deletion mutant,

* Corresponding author. Tel.: +31 15 2785307; fax: +31 15 2782355.
E-mail address: w.a.vanwinden@tnw.tudelft.nl (W.A. van Winden).

1567-1356/$22.00
doi:10.1016/j.femsyr.2004.10.007

grown in aerobic, carbon substrate-limited chemostat cultures on increasing fractions of (partially u-$^{13}C_2$-labeled) acetate.

Maaheimo et al. [3] have performed 2D [^{13}C,^{1}H] correlation nuclear magnetic resonance spectroscopy (COSY NMR) to measure the ^{13}C-distribution in the same *S. cerevisiae* strain CEN.PK113-7D growing exponentially on a mixture of naturally-labeled and u-$^{13}C_6$-labeled glucose in aerobic and anaerobic batch cultures. They used the metabolic-flux ratio analysis (METAFoR) approach to determine flux distributions in a number of convergent metabolic nodes. Fiaux et al. [4] have extended the study by Maaheimo et al. by applying their analytical and computational methods to determine the fluxome of *S. cerevisiae* (and of another eukaryote, *Pichia stipitis*) in aerobic and anaerobic carbon-limited chemostat culture. Blank and Sauer [5] combined GC–MS measurements (similar to [1,2]) with the METAFoR analysis [3,4] to study the effect of temperature, pH, and osmolarity on fluxes in *S. cerevisiae* strain CEN.PK113-7D grown in aerobic batch cultures containing a mixture of naturally-labeled and u-$^{13}C_6$-labeled glucose.

When comparing the flux ratios of five metabolic nodes determined by Gombert et al. [1] with those determined by Maaheimo et al. [3] and by themselves, Fiaux et al. [4] observed good agreement between the chemostat cultures. For batch cultures, the studies give more different results but this may be partially explained by slightly varying experimental conditions. From the consistency of the flux distributions determined for the chemostat cultures using the various methods, Fiaux et al. conclude that the techniques provide reliable results.

In the present study, we present a new liquid chromatography–mass spectrometry (LC–MS)-based approach to determine the ^{13}C-label distribution in a number of intermediates of the central carbon metabolism. We apply this approach to analyse metabolic fluxes in the same CEN.PK113-7D strain of *S. cerevisiae*, grown in an aerobic, carbon-limited chemostat culture. Measurement of the ^{13}C-labeling state of the metabolic intermediates is allowed by rapid sampling and quenching of biomass followed by extraction, separation and very sensitive detection of intermediates of the primary metabolism using LC–MS [6,7]. Until the present, direct measurement of the ^{13}C-labeling distribution of the intermediates of the central carbon metabolism was impeded by their high turnover rates and low concentrations [8,9]. For this reason, in all of the above mentioned studies the ^{13}C-labeling patterns of the intermediates were inferred from NMR and GC–MS measurements of hydrolysates of accumulating biomass components, such as protein and storage carbohydrate that are synthesized from primary metabolites via known or assumed pathways. The method presented here allows a flux fit based on the ^{13}C-labeling data of the intermediates themselves. This method therefore does not rely on assumptions on biosynthetic reaction pathways, such as the absence or presence of multiple alternative pathways to a given amino acid (e.g., glycine stemming either from 3-phosphoglycerate via serine, from oxaloacetate via threonine or from glyoxylate [2]) or compartmentalization of (parts of) the pathways in eukaryotes (e.g., biosynthesis of alanine from cytosolic or mitochondrial pyruvate [2]). Moreover, it gives access to the ^{13}C-labeling pattern of intermediates that are no precursor of biomass components.

Because of the fast turnover of most intracellular metabolite pools, the LC–MS-based assessment of the ^{13}C-labeling distribution in cells also holds the potential practical advantage of allowing for short ^{13}C-labeled medium supply. This is in contrast to NMR- and GC–MS-based ^{13}C-labeling analysis where a much longer time is needed to ^{13}C-label the biomass itself. The attainment of isotopomeric steady-state within a short ^{13}C-labeled medium supply requires the absence of recycling of (unlabeled) biomass components to metabolic precursors, as was for example discussed for proteins in [10].

2. Materials and methods

2.1. Strain and growth conditions

The haploid, prototrophic *S. cerevisiae* strain CEN.PK-113.7D was cultured in an aerobic carbon-limited chemostat culture with a working volume of 4 l in a weight-controlled 7-l fermentor (Applikon Dependable Instruments, Schiedam, The Netherlands). The pH was controlled at pH 5 (BioController ADI 1030, Applikon Dependable Instruments), the temperature was controlled at 30 °C (Thermostat WK 230, Lauda, Lauda-Königshofen, Germany), the stirrer speed was 800 rpm and the aeration rate 0.68 l air/l broth/min. Cultivation proceeded at a constant dilution rate of 0.10 h^{-1}. An overpressure of 0.3 bar was applied to allow rapid sampling. The medium that was supplied was the defined mineral medium as given in [11] with 10 g l^{-1} glucose and 1.0 g l^{-1} ethanol as dual carbon source. Nitrogen was solely provided in the form of ammonia.

Steady-state conditions were routinely checked by off-line measurements of the biomass concentration through filtration on nitro-cellulose filters (pore size 0.45 μm, Gelman Science, Ann Arbor, MI, USA) and by on-line measurements of the off-gas concentrations of O_2 and CO_2 (combined paramagnetic/infrared analyser, NGA 2000, Rosemount Analytics, Santa Clare, CA, USA). Gas flow rates were measured using a Saga Digital Flow Meter (Ion Science, Cambridge, UK). The carbon balance closed within 5%.

When the chemostat culture had reached metabolic steady-state after seven residence times, the unlabeled

medium was replaced by chemically identical medium in which 100% of the glucose was specifically 1-$^{13}C_1$-labeled (D-glucose [1-$^{13}C_1$], CAS: 40762-22-9, Cambridge Isotope Laboratories Inc., Andover, MA, USA) and in which 100% of the ethanol was uniformly ^{13}C-labeled (ethanol [u-$^{13}C_2$], CAS: 70753-79-6, Cambridge Isotope Laboratories Inc., Andover, MA, USA).

2.2. Biomass sampling and sample handling

Biomass samples were taken for LC–MS analysis immediately before and 40 and 60 min after the switch to ^{13}C-labeled medium. Based on literature data on intracellular pool sizes and reaction rates, it had been estimated that of all the primary metabolites the lumped α-ketoglutarate/glutamate-pool had the smallest turnover rate. According to these estimations more than 97% of this intermediate pool is replaced by intermediates formed from the ^{13}C-labeled substrate within 30 min of ^{13}C-labeled medium supply. At each of the three time points (0, 40 and 60 min) 1-ml samples (corresponding to 5 mg of biomass) were taken using the rapid-sampling setup described in [6]. Immediate quenching of the metabolism, separation of the cells from the extracellular liquid, washing and cell extraction were also performed as described in [6]. The ethanol and traces of methanol were removed from the extracted samples in a RapidVap vacuum evaporation system using vacuum along with a temperature gradient and vortex motion (Labconco, Kansas City, MO, USA). During the drying three samples of the same time point were combined into one, to obtain a final amount of biomass of 15 mg per sample. The dried samples were dissolved in 0.5 ml of demineralized water, centrifuged (5 min, 11,000*g*) and decanted to remove insoluble matter. They were stored at −80 °C prior to analysis.

2.3. MS measurements

The metabolic intermediates in the biomass extract were separated by high-performance anion exchange chromatography. This was done using an Alliance pump system (Waters, Milford, USA) followed by an IonPac AS11 (250 × 4 mm) column equipped with an AG11 (50 × 4 mm) precolumn (both from Dionex, Sunnyvale, CA, USA). The flow rate was 1 ml min^{-1}. In all cases 10-μl sample was injected. From the above sample preparation method it follows that 10 μl sample contains the intracellular metabolites originating from 0.30 mg dry weight of *S. cerevisiae*. The sodium hydroxide concentration of the HPLC eluent being too high for a proper mass spectrometric analysis, the sodium cations were exchanged for protons by a post-column ASRS Ultra 4 mm 'Self Regenerating Suppressor' from Dionex. Subsequent MS analyses were performed with a Quattro-LC triple quadrupole mass spectrometer (Micromass Ltd., Manchester, UK). The system is equipped with an electrospray ionization interface with a mass range up to 1600 *m/z*. The nebulizer gas flow (nitrogen) was 75 l h^{-1} and the desolvation gas flow (nitrogen) was 680 l h^{-1}. The source block temperature was 80 °C and the desolvation gas temperature was 250 °C. The capillary voltage was set at −2.7 kV. All samples were analyzed in the negative mode giving $[M-H]^-$ ions, which were monitored in the single-ion recording (SIR) mode with a resolution of 0.8 mass units. For further details regarding the MS method, see [7]. Note that the measured mass isotopomer distributions of the intracellular metabolites are independent of their absolute concentrations. Consequently, the data are not affected by changes in any of the intracellular metabolite concentrations that could occur due to losses in sample handling.

The resulting data are the mass fractions of the following intermediates of the glycolysis and pentose phosphate pathway: glucose 6-phosphate, glucose 1-phosphate, fructose 6-phosphate, fructose 1,6-bisphosphate, 2/3-phosphoglycerate, phosphoenolpyruvate, 6-phosphoglycerate, pentose 5-phosphate, erythrose 4-phosphate and sedoheptulose 7-phosphate. The identity of each of these components was checked against a standard sample.

The peaks of 2-phosphoglycerate and 3-phosphoglycerate are not separated in the chromatography, therefore only their combined mass distribution can be determined. Similarly, the pentose 5-phosphate mass fractions were determined from the overlapping ribose 5-phosphate and ribulose 5-phosphate (and possibly also xylulose 5-phosphate) peaks. Standard deviations of the mass fractions were determined from at least five repeated measurements.

2.4. Metabolic-flux analysis

2.4.1. Metabolic-network model

The studied metabolic network of *S. cerevisiae* is presented in Fig. 1. It includes glycolysis and the pentose phosphate pathway. The metabolic model is a lumped form of the true metabolic network. This lumped network was obtained by applying the network simplification rules proposed in [12] that state that all metabolite pools with only one influx can be removed from the model and that all metabolite pools that may be assumed to be in isotopic equilibrium due to fast exchange reactions can be lumped into one single pool. Bidirectional fluxes are modeled as separate forward and backward fluxes (e.g., v_3 catalyzed by phosphoglucose isomerase) and will in the following be referred to as net and exchange fluxes, where:

$$v_{\text{net}} = v_{\text{forward}} - v_{\text{backward}},$$

$$v_{\text{exchange}} = \min\left(v_{\text{forward}}, v_{\text{backward}}\right).$$

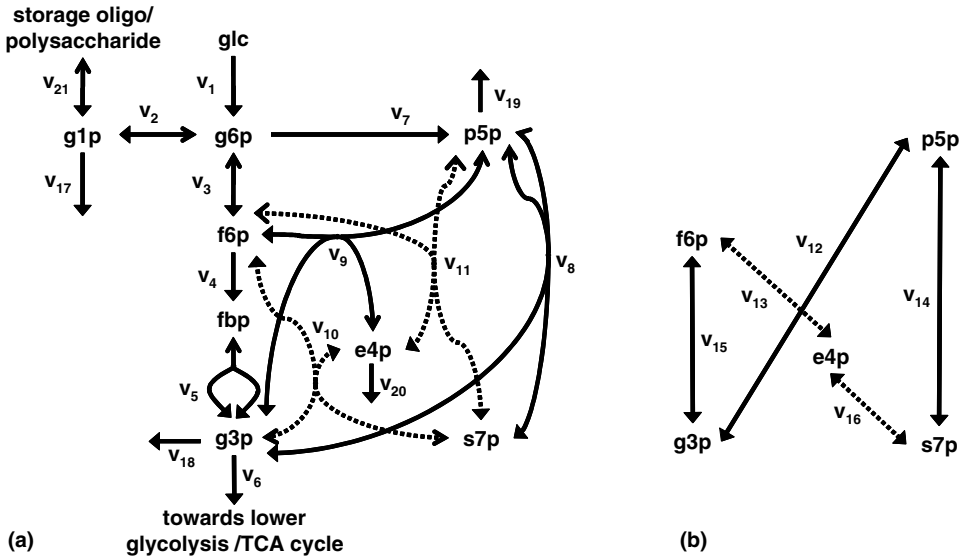

Fig. 1. The metabolic-network model of *S. cerevisiae*. Double-headed arrows indicate reversible fluxes, the solid arrowhead defines the direction of net flux. The sub-network in (b) forms part of the network in (a) and is shown separately for visual clarity. Abbreviations: g6p, glucose 6-phosphate; g1p, glucose 1-phosphate; f6p, fructose 6-phosphate; fbp, fructose 1,6-bisphosphate; g3p, glyceraldehyde 3-phosphate; p5p, pentose 5-phosphate; e4p, erythrose 4-phosphate; s7p, sedoheptulose 7-phosphate.

The non-oxidative branch of the pentose phosphate pathway is the extended version that was proposed in [13]. This network includes one more transketolase reaction (v_{11}), with a nonzero stoichiometry, than the traditional network which only includes v_8–v_{10}. Furthermore, it contains three transketolase reactions (v_{12} through v_{14}) and two transaldolase reactions (v_{15} through v_{16}) that merely exchange two-carbon and three-carbon fragments between two identical couples of metabolites. These reactions have no net stoichiometry, but do influence the ^{13}C-labeling distribution as is explained in [13].

The anabolic consumption of various metabolic intermediates is modeled as effluxes v_{17} to v_{20}, where the effluxes of glucose 6-phopshate and glucose 1-phosphate are lumped into one efflux, v_{17}. The metabolic intermediate glucose-1-phosphate has a reversible flux towards storage carbohydrates (v_{21}). The inclusion of this flux is indispensable for the fitting of the observed mass fractions of this intermediate as will be explained in Section 3.

2.4.2. Flux fitting

In order to analyze the number of free fluxes in the metabolic network model, the stoichiometry matrix (S) is combined with measurement matrix (R) that contains a row with a unity entry for each (indirectly) measured net conversion rate. The combined stoichiometry and measurement matrices are used to find a generalized solution (v) for the under determined flux balances as described in [12]

$$\mathbf{v} = \begin{pmatrix} \mathbf{S} \\ \mathbf{R} \end{pmatrix}^{\#} \cdot \begin{pmatrix} \mathbf{0} \\ \mathbf{v}_{\mathrm{m}} \end{pmatrix} + \mathrm{null}\begin{pmatrix} \mathbf{S} \\ \mathbf{R} \end{pmatrix} \cdot \beta, \qquad (1)$$

where '#' denotes the pseudo inverse and 'null' the null space of the combined stoichiometry and measurement matrix. The first term in the generalized flux solution in Eq. (1) is fully determined by the influx and effluxes (v_{m}) of the metabolic network that are determined from the measured net conversion rates. The second term is a linear combination of the columns that span the null space of the full set of flux balances. The vector β contains the free flux parameters that need to be fitted to the measured ^{13}C-labeling data.

The free flux parameters are fitted in an iterative fashion by substituting a set of parameter values in Eq. (1) and using the resulting set of fluxes as input for the cumomer balances [14] of the metabolic network of Fig. 1. The calculated cumomers are transformed to the actually measured ^{13}C-labeling data as explained in [14,15]. The variance-weighted sum of squared deviations between the simulated and measured data is used as the target function in a minimization procedure based on sequential quadratic programming that was implemented in Matlab (The MathWorks Inc., Natick, MA, USA). The flux-fitting software can be obtained from the corresponding author upon request.

3. Results and discussion

3.1. Evaluation of measured mass isotopomer distributions

Table 1 (columns 'measured') gives the mass fractions of 10 metabolic intermediates that were measured in the extracts of the biomass that was sampled 0, 40 and 60

Table 1
Measured and fitted mass fractions and standard deviations of intermediates of glycolysis and pentose phosphate pathway

Measured compound	Mass fraction	Sample				
		Measured, time = 0 min	Calculated, time = 0 min	Measured, time = 40 min	Measured, time = 60 min	Fitted, time = 60 min
G6P ($M = 259$)	$M+0$	0.911 ± 0.007	0.916	0.174 ± 0.009	0.192 ± 0.015	0.193
	$M+1$	0.065 ± 0.005	0.064	0.721 ± 0.010	0.697 ± 0.013	0.696
	$M+2$	0.022 ± 0.002	0.019	0.085 ± 0.010	0.092 ± 0.010	0.092
	$M+3$			0.019 ± 0.002	0.020 ± 0.002	0.017
G1P ($M = 259$)	$M+0$	0.910 ± 0.005	0.916	0.306 ± 0.040	0.332 ± 0.027	0.313
	$M+1$	0.064 ± 0.004	0.064	0.637 ± 0.039	0.610 ± 0.021	0.592
	$M+2$	0.025 ± 0.006	0.019	0.057 ± 0.009	0.059 ± 0.016	0.080
F6P ($M = 259$)	$M+0$	0.910 ± 0.009	0.916	0.189 ± 0.020	0.202 ± 0.033	0.197
	$M+1$	0.067 ± 0.005	0.064	0.711 ± 0.021	0.684 ± 0.038	0.689
	$M+2$	0.021 ± 0.005	0.019	0.082 ± 0.008	0.092 ± 0.012	0.095
	$M+3$			0.017 ± 0.003	0.021 ± 0.001	0.017
	$M+4$			0.002 ± 0.002	0.001 ± 0.001	0.002
F16BP ($M = 339$)	$M+0$	0.893 ± 0.015	0.909	0.330 ± 0.016	0.350 ± 0.027	0.351
	$M+1$	0.077 ± 0.013	0.065	0.522 ± 0.026	0.496 ± 0.026	0.498
	$M+2$	0.029 ± 0.003	0.024	0.125 ± 0.013	0.127 ± 0.015	0.130
	$M+3$			0.021 ± 0.002	0.023 ± 0.002	0.018
	$M+4$			0.002 ± 0.002	0.004 ± 0.001	0.003
2/3PG ($M = 185$)	$M+0$	0.950 ± 0.004	0.951	0.640 ± 0.012	0.628 ± 0.016	0.632
	$M+1$	0.035 ± 0.002	0.034	0.331 ± 0.013	0.343 ± 0.016	0.345
	$M+2$	0.015 ± 0.001	0.014	0.022 ± 0.002	0.022 ± 0.001	0.018
	$M+3$			0.006 ± 0.002	0.007 ± 0.000	0.005
PEP ($M = 167$)	$M+0$	0.952 ± 0.001	0.954	0.630 ± 0.015	0.631 ± 0.020	0.634
	$M+1$	0.035 ± 0.001	0.034	0.340 ± 0.013	0.338 ± 0.021	0.345
	$M+2$	0.013 ± 0.001	0.012	0.023 ± 0.002	0.024 ± 0.002	0.017
	$M+3$			0.007 ± 0.001	0.007 ± 0.001	0.004
6PG ($M = 275$)	$M+0$	0.915 ± 0.003	0.914	0.199 ± 0.008	0.195 ± 0.006	0.192
	$M+1$	0.065 ± 0.003	0.064	0.701 ± 0.009	0.698 ± 0.006	0.695
	$M+2$	0.019 ± 0.001	0.021	0.086 ± 0.003	0.096 ± 0.004	0.093
	$M+3$			0.014 ± 0.001	0.011 ± 0.006	0.018
P5P ($M = 229$)	$M+0$	0.941 ± 0.002	0.928	0.745 ± 0.009	0.758 ± 0.012	0.756
	$M+1$	0.051 ± 0.001	0.054	0.219 ± 0.007	0.202 ± 0.012	0.202
	$M+2$			0.034 ± 0.003	0.037 ± 0.004	0.038
	$M+3$			0.002 ± 0.001	0.003 ± 0.003	0.004
E4P ($M = 199$)	$M+0$	0.948 ± 0.003	0.941	0.866 ± 0.004	0.866 ± 0.005	0.862
	$M+1$	0.045 ± 0.002	0.044	0.122 ± 0.004	0.123 ± 0.005	0.119
	$M+2$			0.013 ± 0.002	0.012 ± 0.003	0.017
S7P ($M = 289$)	$M+0$	0.896 ± 0.006	0.904		0.483 ± 0.013	0.480
	$M+1$	0.079 ± 0.004	0.073		0.395 ± 0.014	0.398
	$M+2$	0.023 ± 0.002	0.021		0.106 ± 0.007	0.101
	$M+3$				0.016 ± 0.001	0.019

min after the switch from naturally-labeled medium to ^{13}C-labeled medium.

3.1.1. Mass isotopomer fractions of naturally-labeled biomass

The mass fractions of the sample taken at $t = 0$ represent the ^{13}C-labeling distribution of metabolites formed from naturally-labeled glucose and ethanol. The mass fractions greater than $M+0$ are caused by naturally-occurring isotopes of carbon, oxygen and hydrogen. In the cumomer model used to simulate the mass isotopomer fractions, the natural occurrence of the ^{13}C-isotope is taken into account when defining the cumomer distribution of the carbon substrates. The occurrence of natural isotopes of the atom species other than carbon is accounted for by applying the correction procedure proposed in [16].

The cumomer model can be used to generate the mass isotopomers of all metabolic intermediates formed from naturally-labeled carbon substrates by setting the ^{13}C-labeled fractions of the substrates at zero. These calculated mass isotopomer fractions can be compared to

the corresponding measured mass isotopomer fractions of the sample taken at $t = 0$. Since these mass isotopomer fractions are fully independent of both the topology of the metabolic reaction network and of the fluxes therein, this comparison allows verification of the accuracy of the mass isotopomer measurements. Table 1 (column 'calculated, time = 0 min') shows that the calculated fractions agree well with the measured ones. Seeing the small standard deviations of the mass fractions, the observed correspondence between the measured and theoretically expected values at $t = 0$ demonstrates the accuracy of the MS measurements.

3.1.2. Mass isotopomer fractions of biomass grown on 1-$^{13}C_1$-glucose

The biomass was sampled both at $t = 40$ and at $t = 60$ min in order to check whether the ^{13}C-labeling distributions of the intracellular metabolites were in isotopic steady-state after more than 30 minutes, as was estimated on the basis of literature values of intracellular pool sizes and estimated fluxes. It can be verified in Table 1 (columns 'measured, time = 40 and 60') that the mass fractions do not change significantly after 40 min, indicating that these metabolic intermediates may indeed be assumed in isotopic steady-state.

The similarity of the mass isotopomer fractions in the two independently sampled, washed, extracted and analyzed biomass samples ($t = 40$, respectively, $t = 60$) further indicates that the procedure is reproducible. If the metabolism were not instantaneously quenched and turnover of metabolites would still occur in an uncontrolled way in the sampled biomass, the outcomes of the two samples would very unlikely show the same consistency.

Inspecting the mass isotopomer distributions further shows that prior to any calculation, the distributions already hold information on the metabolic fluxes. For example: the near-identity of the mass fractions of glucose 6-phosphate and fructose 6-phosphate at $t = 40$ and $t = 60$ demonstrates that either fructose 6-phosphate is uniquely synthesized from glucose 6-phosphate or, in case the fructose 6-phosphate pool has additional influxes, that the phosphoglucose isomerase catalyzes an exchange flux that is considerably larger than its net flux. Under the current experimental conditions, it is to be expected that part of the glucose will be converted via the pentose phosphate pathway. By consequence, fructose 6-phosphate will have influxes catalyzed by transaldolase and transketolase (v_9 through v_{11}, v_{13} and v_{15} in Fig. 1), suggesting that the phosphoglucose isomerase reaction is highly reversible.

No such large exchange flux is found for phosphoglucomutase that interconverts glucose 6-phosphate and glucose 1-phosphate. The latter metabolite has a larger $M + 0$ fraction and lower $M + 1$ and $M + 2$ fractions than glucose 6-phosphate, which indicates that the reaction between the two components is not at equilibrium. A tentative explanation for the fact that glucose 1-phosphate is ^{13}C-labeled to a lower extent than glucose 6-phosphate is that the glucose 1-phosphate that stems from glucose 6-phosphate is diluted by glucose 1-phosphate molecules that originate from turnover of the large intracellular glycogen pool, which is not yet in isotopic steady-state after 40 and 60 min of ^{13}C-labeled medium supply. This explanation is supported by the finding of Mashego et al. [17] who switched a chemostat culture of the same strain from naturally-labeled to 100% uniformly ^{13}C-labeled feed and observed that the fraction of remaining unlabeled glucose 1-phosphate rapidly decreased, but leveled off and stayed constant at around 20% during several hours after the onset of ^{13}C-labeled feeding.

The occurrence of simultaneous glycogen synthesis and degradation is in fact a futile cycle, wasting ATP. The occurrence of this phenomenon in *S. cerevisiae* was discussed by François and Parrou [18] who suggested that it could act as a 'glycolytic safety valve' preventing death of the cells by ATP imbalance under stress conditions. It remains an open question why glycogen cycling would then occur under the undisturbed conditions of the present study.

Because of the suspected influx of unlabeled glucose 1-phosphate, the apparent isotopic steady-state within 40 min is in fact not truly steady: it will take considerably more time before the glycogen storage pool will be in true isotopic steady-state. In the model, the continuing turnover of partially unlabeled glycogen that dilutes the ^{13}C-labeling of the glucose 1-phosphate pool is accounted for by adding an influx with unlabeled compound ($v_{21\,f}$) and an equally large efflux ($v_{21\,b}$) of the same pool.

From the data in Table 1 it can furthermore be inferred that the reactions interconverting fructose 1,6-bisphosphate and two molecules of 2/3-phosphoglycerate are not in equilibrium. The mass isotopomer distribution of fructose 1,6-bisphosphate that can be calculated by multiplying two mass isotopomer distributions of 2/3-phosphoglycerate at $t = 60$ is: $M + 0 = 0.394$, $M + 1 = 0.431$ and $M + 2 = 0.145$. This does not correspond very well to the actually measured values, as should be the case at equilibrium.

The mass isotopomer fractions of the combined 2/3-phosphoglycerate pool are very similar to those of phosphoenolpyruvate at both $t = 0$ and $t = 60$. This demonstrates that the phosphoglycerate mutase and enolase also catalyze exchange fluxes that are significantly higher than the net glycolytic flux.

Finally, the good agreement of the glucose 6-phosphate and 6-phosphogluconate metabolites that is observed in Table 1 serves as a quality control, as in *S. cerevisiae* the latter compound uniquely originates from the former, and thus must have an identical ^{13}C-label distribution.

3.2. ^{13}C-labeling-based metabolic-flux analysis

3.2.1. Macroscopic measurements of fermentation

Table 2 shows the biomass-specific extracellular rates, biomass concentration, dissolved oxygen level, respiratory quotient and biomass yield of the chemostat culture. The net conversion rates of the studied metabolic network in Fig. 1 (v_1 and v_{17} through v_{20}) were derived from the data in Table 2 by balancing according to [19], using the detailed metabolic model in [20]. All fluxes are normalized (on mole base) to a glucose influx (v_1) of 100.

3.2.2. Fitting measured mass isotopomer fractions of biomass grown on 1-$^{13}C_1$-glucose

The metabolic fluxes, which are constrained by the measured net conversion rates following Eq. (1), were determined by fitting simulated mass fractions to the measured mass isotopomer fractions of metabolites extracted from the biomass that was sampled at $t = 60$. Only mass isotopomer fractions larger than 0.03 were fitted as it was observed that fitting very small mass isotopomer fractions leads to a considerable increase of the minimized sum of squared errors. This may be explained by the fact that the standard deviations used in the error-weighted fitting only account for the measurement inaccuracy of the LC–MS. Any systematic modeling error, albeit small, will lead to large error-weighted contributions of small mass fractions. Note that because the mass isotopomer fractions of each intermediate sum up to one, one fraction per metabolite holds no independent information. Therefore, omission of 9 out of the 13 mass isotopomer fractions smaller than 0.03 did not lead to a loss of information.

When fitting the measured mass isotopomer fractions the substrate (i.e., glucose)-labeling was defined in the model as 100% ^{13}C-labeled on the first carbon position and naturally-^{13}C-labeled on the remaining five carbon positions of the molecule. Notably, our initial erroneous assumption of unique ^{13}C-labeling on the first carbon position led to a larger minimized sum of squared deviations and significantly different estimated metabolic fluxes (results not shown).

Table 2
Macroscopic measurements and yields of the chemostat culture

Glucose consumption	(mmol/g biomass/h)	0.94 ± 0.01
Ethanol consumption	(mmol/g biomass/h)	0.40 ± 0.01
Oxygen consumption	(mmol/g biomass/h)	2.87 ± 0.06
Carbondioxide production	(mmol/g biomass/h)	2.64 ± 0.06
Biomass production	(1/h)	0.10 ± 0.002
Dissolved oxygen	(% of saturation level)	60 ± 5
Biomass concentration	(g/l)	5.33 ± 0.05
Respiratory quotient	(mol/mol)	0.92 ± 0.03
Yield(biomass/glucose+ethanol)	(C-mol/C-mol)	0.58 ± 0.01

The optimally-fitted mass fractions are shown in Table 1 (column 'fitted, time = 60 min'). The fitted values agree very well with the measured values; the mean absolute deviation between the measured and fitted mass isotopomer fractions is 0.004, the maximum deviation is 0.021. The minimized covariance weighted sum of squared residuals of the fit is 6.5. This sum is a χ^2-distributed variable with a statistical expectation equal to the number of independent data points minus the number of model parameters. In the above case 26 independent mass fractions larger than 0.03 are fitted by 16 parameters, therefore the statistical expectation of the sum of squared residuals is 10. The fit of the measured mass isotopomer fractions is clearly statistically acceptable.

Fitting same data with the traditional metabolic network excluding the additional transketolase and transaldolase reactions discussed in Section 2.4.1. led to a minimized covariance-weighted sum of squared residuals of 110.1. This model had nine free flux parameters and thus fitted $26 - 9 = 17$ independent data points. The negligible probability $\chi^2(110.1, 17)$ leads us to reject the hypothesis that the traditional model is correct.

The metabolic fluxes corresponding to the optimal fit of the statistically accepted model are shown in Fig. 2. As was already inferred from the inspection of the mass fractions in Section 3.1.2, the phosphoglucose isomerase reaction is highly reversible. Both the phosphoglucomutase and the fructose bisphosphate aldolase reactions are reversible, but their exchange reactions are not high enough to fully equilibrate the ^{13}C-label distributions of their respective substrates and products. The reactions catalyzed by transketolase and transaldolase show a varying extent of reversibility. In the present study it was not investigated how reliably fluxes in the non-oxidative branch of the pentose phosphate pathway can be determined from the available data.

Fig. 2 shows that the split ratio of glucose towards the pentose phosphate pathway, which is hereby defined as v_7/v_1, was estimated to be 0.24. From Table 2 it can be calculated that per mole of glucose and 0.42 mol of ethanol that is co-consumed, 106 g of biomass is formed. Assuming that the biosynthesis of 100 g of biomass from glucose requires 0.88 mol of NADPH [1, references therein], 106 g of biomass requires 0.94 mol of NADPH for its formation. When it is furthermore assumed that the 0.42 mol of ethanol enters the metabolism via NADP-dependent acetaldehyde dehydrogenase, the remaining $0.94 - 0.42 = 0.52$ mol of NADPH has to be generated from 1 mol of glucose. Neglecting possible alternative sources of NADPH (such as NADP-dependent isocitrate dehydrogenase), the estimated fraction of glucose that needs to be converted via the oxidative branch of the pentose phosphate pathway is $0.52/2 = 0.26$, i.e., close to the value estimated in this study.

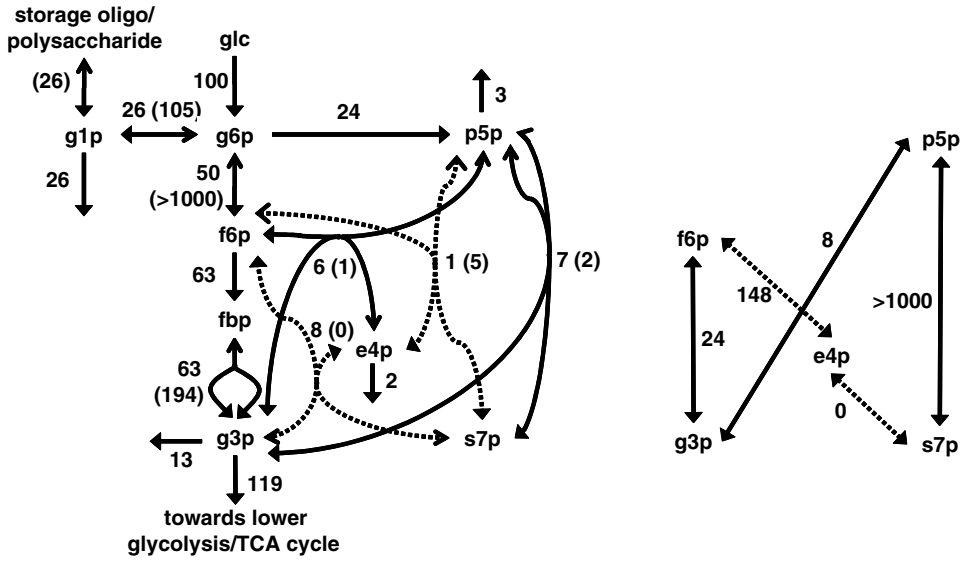

Fig. 2. The metabolic fluxes of *S. cerevisiae* growing in a carbon-limited, aerobic chemostat culture at $D = 0.1$ h as determined by fitting the mass isotopomer fractions measured by LC–MS in biomass sampled 60 min after the shift to ^{13}C-labeled medium. Values outside brackets represent net fluxes, the direction of the positive net flux being defined by the solid arrowhead. The values within brackets present exchange fluxes. Abbreviations: see Fig. 1.

The split ratio of 0.24 found here is considerably lower than the split ratio of 0.44 found by Gombert et al. [1]. However, the difference may be at least partially attributable to the NADPH generated from the ethanol in the medium as was discussed before. Ethanol was absent in the medium used in [1].

3.2.3. Confidence interval of pentose phosphate pathway split ratio

In order to further study the difference between the flux towards the pentose phosphate pathway reported here and the one determined by Gombert et al. [1] we determined the confidence interval of the split ratio. The model that relates the metabolic fluxes to the mass isotopomer fractions is highly non-linear, which makes the commonly applied estimation of a confidence interval based on linearization of the model around the optimally fitted fluxes prone to errors. Therefore, an approach was chosen where the split ratio was subsequently fixed at all values between 0.04 and 0.60 with intervals of 0.05, and the remaining degrees of freedom were re-fitted. In Fig. 3 the resulting minimized variance-weighted sums of squared residuals are plotted versus the fixed split ratio. A striking feature of this plot is the flat profile of the curve in a considerable range of split ratios around the optimally fitted value.

The plot also shows the line indicating the minimized sum of squared residuals that corresponds to the 90% confidence interval ($\chi^2(16.0, 17) = 0.9$). For all fits below this line the chance that the minimized sum of squared residuals results only from random measurement errors is 10% or larger. The figure shows that the split ratio lies

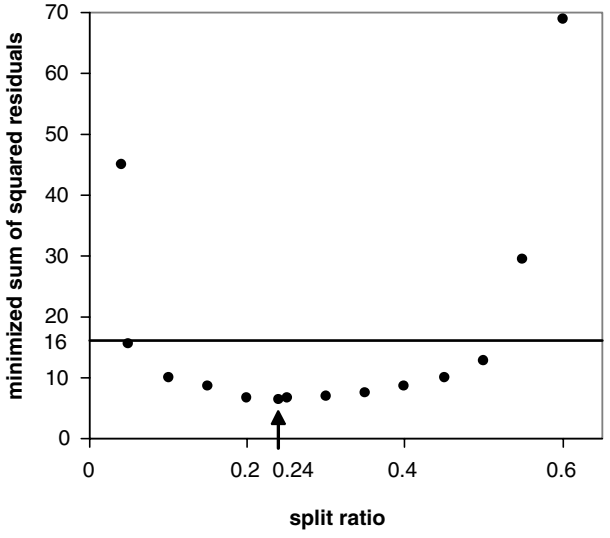

Fig. 3. The minimized sum of squared errors plotted against the fixed pentose phosphate pathway split ratio (•). The solid line represents the 90%-confidence interval of the $\chi^2(10)$-distributed sum of squared residuals (see Section 3.2.3). The arrow indicates the optimally-fitted split ratio.

between 0.05 and 0.52 at a confidence level of 90%. Note that the split ratio found in [1] lies within this confidence interval.

When inspecting the sets of fluxes fitted for all fixed split ratios within the confidence interval, it was found that the storage carbohydrate turnover rate has a close, negative correlation with the split ratio. In other words: the larger the flux into the pentose phosphate pathway (v_7), the smaller the estimated unlabeled carbohydrate

turnover (v_{21}). This can be understood when it is realized that the ^{13}C-labeling on the first carbon position of glucose 6-phosphate is lost by decarboxylation to pentose 5-phosphate in the oxidative branch of the pentose phosphate pathway. A decreasing inflow of unlabeled hexose phosphates into the metabolism via the reversible storage carbohydrate turnover (v_{21}), phosphoglucomutase (v_2) and phosphoglucose isomerase (v_3) reactions compensates for this increasing loss of ^{13}C via the pentose phosphate pathway. Indeed, when the fits shown in Fig. 3 were redone with a carbohydrate turnover that was fixed at its value found for the optimal fit, it was observed that the minimized sums of squared residuals increased much steeper around the optimal fit (results not shown).

4. Conclusions

In this study we demonstrated the potential of a new method for ^{13}C-labeling analysis based on rapid sampling and quenching of microorganisms from a cultivation, followed by extraction and detection by liquid chromatography-mass spectrometry of free intracellular metabolites. The method was successfully applied to *S. cerevisiae* for ^{13}C-labeling-based metabolic flux analysis of the glycolysis and pentose phosphate pathway.

The presented LC–MS-based ^{13}C-labeling analysis has clear advantages. In contrast to GC–MS and NMR, it yields ^{13}C-labeling information on metabolites that do not serve as a precursor for biosynthesis of accumulating compounds, such as proteinogenic amino acids. Metabolites of which the ^{13}C-labeling was made accessible for the first time here are fructose 1,6-bisphosphate, 2/3-phosphoglycerate, 6-phosphogluconate and sedoheptulose 7-phosphate.

The approach yields direct information on reaction reversibility by comparing measured mass isotopomer fractions of substrates and products of monomolecular reactions. The results in this study showed that the reactions catalyzed by phosphoglucose isomerase, phosphoglycerate mutase and enolase are highly reversible.

One of the advantages of measuring the distribution of ^{13}C-labeling in intracellular metabolites is that the fast turnover of their small pools would allow a short ^{13}C-labeled feed supply to reach isotopomeric steady-state. In this study ^{13}C-labeled medium was supplied for only 60 min. Isotopomeric steady-state was, however, not attained due to turnover of large unlabeled intracellular storage pools: an unlabeled inflow, likely stemming from glycogen, diluted the ^{13}C-labeling of the glucose 1-phosphate pool. The occurrence of turnover could be taken into account in the model used for flux analysis.

The split ratio towards the pentose phosphate pathway found in this study amounts to 24% of the glucose that enters the cell. This value is lower than that found in a previous study where full isotopomer modeling was applied to fit GC–MS data of the same strain grown under similar conditions. However, the main difference between the two studies, the presence of the co-substrate ethanol in the medium used in this study, may explain the difference as the oxidation of ethanol to acetate is an alternative source of NADPH, which is otherwise predominantly generated by the pentose phosphate pathway.

As the split ratio towards the pentose phosphate pathway is one of the key parameters of the presented metabolic-flux analysis, we determined the reliability of its estimated value. It was found that over a broad range of fixed split ratios the remaining degrees of freedom of the model still allow an acceptable fit of the data. The 90%-confidence interval of the split ratio was determined to be [0.05–0.52]. The cause of the large confidence interval was found to be the storage carbohydrate turnover added to the model. A longer ^{13}C-labeled medium supply than used in this study will prevent the isotopomeric non-steady-state due to this turnover process and thus remove this degree of freedom from the model. It is anticipated that this will result in a smaller confidence interval of the fitted split ratio.

References

[1] Gombert, A.K., Moreira dos Santos, M., Christensen, B. and Nielsen, J. (2001) Network identification and flux quantification in the central metabolism of *Saccharomyces cerevisiae* under different conditions of glucose repression. J. Bacteriol. 183, 1441–1451.

[2] Dos Santos, M.M., Gombert, A.K., Christensen, B., Olsson, L. and Nielsen, J. (2003) Identification of in vivo enzyme activities in the cometabolism of glucose and acetate by *Saccharomyces cerevisiae* by using ^{13}C-labeled substrates. Eukar. Cell 2, 599–608.

[3] Maaheimo, H., Fiaux, J., Çakar, Z.P., Bailey, J.E., Sauer, U. and Szyperski, T. (2001) Central carbon metabolism of *Saccharomyces cerevisiae* explored by biosynthetic fractional ^{13}C-labeling of common amino acids. Eur. J. Biochem. 268, 2464–2479.

[4] Fiaux, J., Çakar, Z.P., Sonderegger, M., Wüthrich, K., Szyperski, T. and Sauer, U. (2003) Metabolic flux profiling of the yeasts *Saccharomyces cerevisiae* and *Pichia stipitis*. Eukar. Cell 2, 170–180.

[5] Blank, L. and Sauer, U. (2004) TCA cycle activity in *Saccharomyces cerevisiae* is a function of the environmentally determined specific growth and glucose uptake rates. Microbiology 150, 1085–1093.

[6] Lange, H.C., Eman, M., van Zuijlen, G., Visser, D., van Dam, J.C., Frank, J., Texeira de Mattos, M.J. and Heijnen, J.J. (2001) Improved rapid sampling for in vivo kinetics of intracellular metabolites in *Saccharomyces cerevisiae*. Biotechnol. Bioeng. 75, 406–415.

[7] van Dam, J.C., Eman, M.R., Frank, J., Lange, H.C., van Dedem, G.W.K. and Heijnen, J.J. (2002) Analysis of glycolytic intermediates in *Saccharomyces cerevisiae* using anion exchange chromatography and electrospray ionization with tandem mass spectrometric detection. Anal. Chim. Acta 460, 209–218.

[8] Szyperski, T. (1998) ^{13}C-NMR, MS and metabolic flux balancing in biotechnology research. Quart. Rev. Phys. 31, 41–106.
[9] Dauner, M. and Sauer, U. (2000) GC–MS analysis of amino acids rapidly provides rich information for isotopomer balancing. Biotechnol. Prog. 16, 642–649.
[10] Grotkjaer, T., Åkeson, M., Christensen, B., Gombert, A.K. and Nielsen, J. (2004) Impact of transamination reactions and protein turnover on labeling dynamics in ^{13}C-labeling experiments. Biotechnol. Bioeng. 86, 209–216.
[11] Verduyn, C., Postma, E., Scheffers, W.A. and van Dijken, J.P. (1992) Effect of benzoic acid on metabolic fluxes in yeasts: a continuous culture study on the regulation of respiration and alcoholic fermentation. Yeast 8, 501–517.
[12] van Winden, W.A., Heijnen, J.J., Verheijen, P.J.T. and Grievink, J. (2001) A priori analysis of metabolic flux identifiability from ^{13}C-labeling data. Biotechnol. Bioeng. 74, 505–516.
[13] van Winden, W.A., Verheijen, P.J.T. and Heijnen, J.J. (2001) Possible pitfalls of flux calculations based on ^{13}C-labeling. Metabol. Eng. 3, 151–162.
[14] Wiechert, W., Möllney, M., Isermann, N., Wurzel, M. and de Graaf, A.A. (1999) Bidirectional reaction steps in metabolic networks: III. Explicit solution and analysis of isotopomer labeling systems. Biotechnol. Bioeng. 66, 69–85.
[15] Möllney, M., Wiechert, W., Kownatzki, D. and de Graaf, A.A.. (1999) Bidirectional reaction steps in metabolic networks: IV. Optimal design of isotopomer labeling experiments. Biotechnol. Bioeng. 66, 86–103.
[16] van Winden, W.A., Wittmann, C., Heinzle, E. and Heijnen, J.J. (2002) Correcting mass isotopomer distributions for naturally occurring isotopes. Biotechnol. Bioeng. 80, 477–479.
[17] Mashego, M.R., Wu, L., van Dam, J.C., Ras, C., Vinke, J.L., van Winden, W.A., van Gulik, W.M. and Heijnen, J.J. (2004) Miracle: mass isotopomer analysis of ^{13}C-labeled extracts. A new method for accurate quantification of changes of concentrations of intracellular metabolites. Biotechnol. Bioeng. 85, 620–628.
[18] François, J. and Parrou, J.L. (2001) Reserve carbohydrates metabolism in the yeast *Saccharomyces cerevisiae*. FEMS Microbiol. Rev. 25, 125–145.
[19] van der Heijden, R.T.J.M., Heijnen, J.J., Hellinga, C., Romein, B. and Luyben, K.Ch.A.M. (1994) Linear constraint relations in biochemical reaction systems: I. Classification of the calculability and the balanceability of conversion rates. Biotechnol. Bioeng. 43, 3–10.
[20] Lange, H.C. (2002) Quantitative Physiology of *Saccharomyces cerevisiae* using Metabolic Network Analysis. PhD-dissertation Delft University of Technology, Delft, The Netherlands.